Supplementary Information

Transduction between magnets and ions

Yecheng Wang[a], Shejuan Xie[b], Yang Bai[b], Zhigang Suo*[a] and Kun Jia*[b]

[a]*John A. Paulson School of Engineering and Applied Sciences, Kavli Institute for Bionano Science and Technology, Harvard University, Cambridge, MA 02138, United States*

[b]*State Key Laboratory for Strength and Vibration of Mechanical Structures, School of Aerospace Engineering, Xi'an Jiaotong University, Xi'an 710049, China*

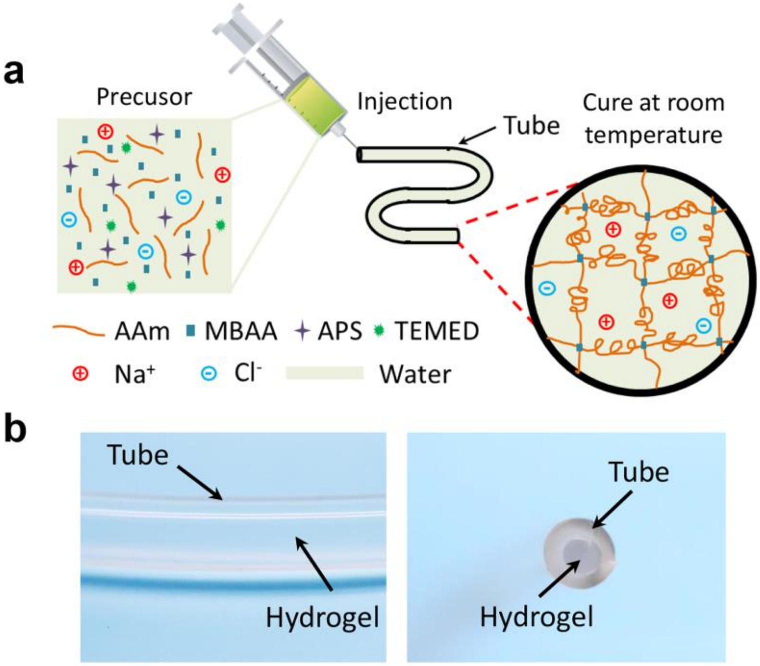

Fig. S1 Schematic for preparation of polyacrylamide hydrogel coil. (a) The precursor was prepared by dissolving acrylamide (AAm, 2 mol L^{-1}) as the monomer, sodium chloride (0.02 mol L^{-1}, 0.2 mol L^{-1}, or 2 mol L^{-1}) as the ionic charge carrier, *N,N'*-methylenebisacrylamide (MBAA, 0.1% the weight of AAm) as the crosslinker, *N,N,N',N'*-tetramethylethylenediamine (TEMED, 0.1% the weight of AAm) as the catalyst, and ammonium persulfate (APS, 0.17% the weight of AAm) as the initiator in deionized water. The precursor solution of the hydrogel was injected into the dielectric tube slowly from one end of the tube until the precursor solution flowed out from the other end. After the injection, no air bubble was observed in the tube by naked eye. The tube filled with the precursor was clamped at its two ends for curing at room temperature for 8 hours. After curing, silver wires were inserted into the two ends of the hydrogel coil and were sealed by Ecoflex 00-30 (Smooth-on; 1:1 base-to-curing agent weight ratio). (b) Photos of the hydrogel coil.

Spatial distribution of the generated electromagnetic field around a metal coil

To determine the spatial distribution of the electromagnetic field around a metal coil, we solve the governing equations in the frequency domain

$$\nabla \times \boldsymbol{H} = \boldsymbol{J}$$

$$\nabla \times \boldsymbol{A} = \boldsymbol{B}$$

$$-\mathrm{i}\omega \boldsymbol{A} = \boldsymbol{E}$$

$$\boldsymbol{B} = \mu \boldsymbol{H}, \tag{S1}$$

where $\boldsymbol{H}$ is the magnetic field, $\boldsymbol{B}$ is the magnetic flux density, $\boldsymbol{J}$ is the current density, $\boldsymbol{A}$ is the magnetic vector potential, μ is the permeability, $\boldsymbol{E}$ is the electric field, ω is the angular frequency, and $\mathrm{i} = \sqrt{-1}$. A finite element method (FEM) software, COMSOL Multiphysics, is used. We apply a sinusoidal current to a copper coil. The effective amplitude and frequency of the current are 150 A and 162 kHz. Due to the geometrical asymmetry of the copper coil (Fig. S2a), we solve the boundary value problem in three dimensions covering an air domain with a length of 400 mm, a width of 100 mm, and a height of 100 mm. We adopt magnetic insulations as the boundary conditions for the air domain. The origin of the coordinate coincides with the center of the copper coil, and *x*, *y*, and *z* axes correspond to the length, width, and height of the air domain. The default material properties of air and copper in the material library are used in the calculation.

We first calculate the spatial distribution of the magnetic field around the copper coil (Fig. S2b and c). The *z*-axis component of the magnetic flux density $\boldsymbol{B}$ in the *x*-*y* plane at *z*=0 reaches maximum at the center region (Fig. S2d).

Next, we calculate the spatial distribution of the electric field around the copper coil (Fig. S2e and f) and show the electric field is asymmetric with respect to the *y*-axis by calculating the *x*-axis component of the electric field $\boldsymbol{E}_{x}$ in the *x*-*y* plane at *z*=0 (Fig. S2g). The electric field varies with the integral lines P0, P1, and P2 (Fig. S2f) in the *x*-*y* plane (Fig. S2g). Although the magnitude of $\boldsymbol{E}_{x}$ along line P2 is smaller than that along line P0, $\boldsymbol{E}_{x}$ along line P2 has higher asymmetry, generating a higher voltage. Furthermore, we calculate $\boldsymbol{E}_{x}$ along line P2 as a function of distance away from the copper coil (Fig. S2i). The electric field decrease as the distance increases, which has similar trends as voltages measured by experiment (Fig. 2e).

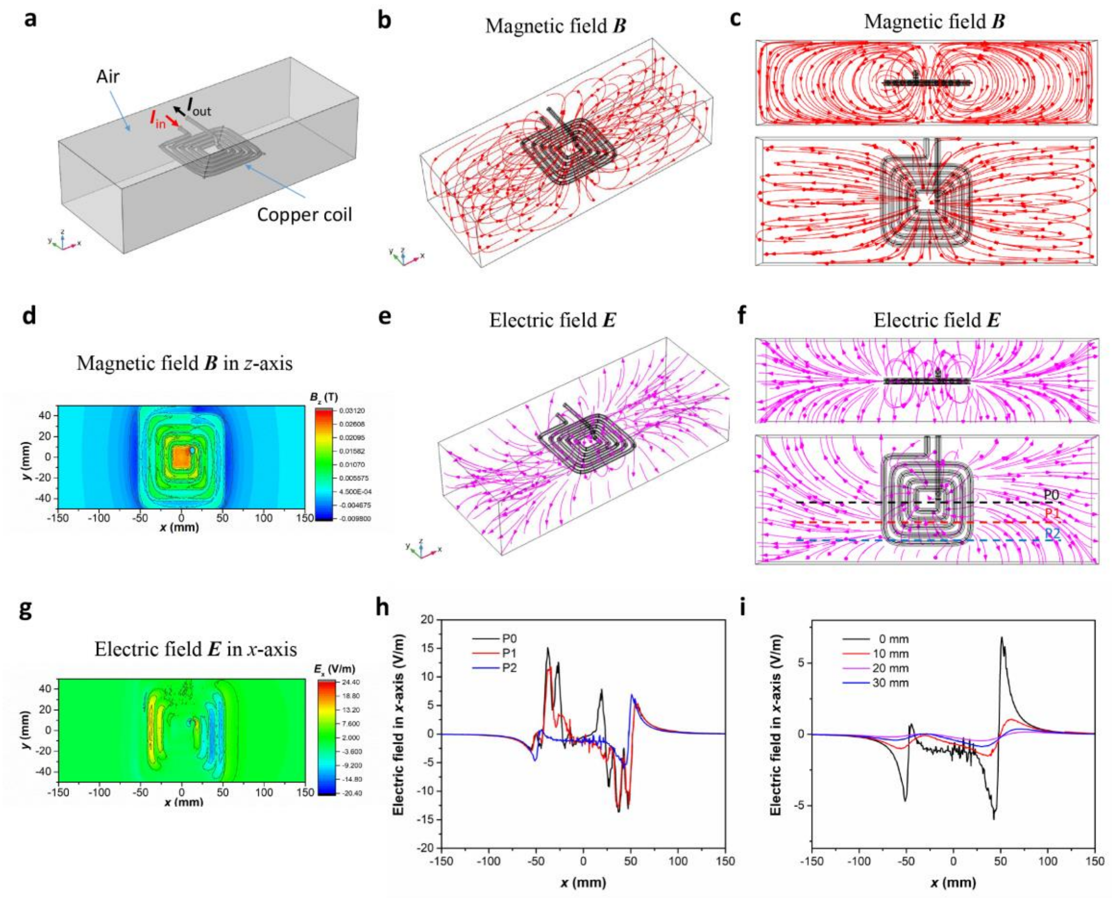

Fig. S2 Finite element analysis on the electromagnetic field generated by a copper coil. (a) Geometrical model used in the FEM analysis. Spatial distribution of the magnetic field around the copper coil in three dimensions (b) and from the top view (c). (d) *z*-axis component of the magnetic flux density in the *x*-*y* plane at *z*=0. Spatial distribution of the electric field around the copper coil in three dimensions (e) and from the top view (f). Three integral lines, P0, P1, and P2, are marked in the top view of the distribution of the electric field. (g) *x*-axis component of the electric field in the *x*-*y* plane at *z*=0. (h) *x*-axis component of the electric field varies with integral lines. Each line integral gives a voltage. (i) *x*-axis component of the electric field along line P2 as a function of distance away from the copper coil.

Energy conversion efficiency of the ionotronic transformer

In the ionotronic transformer, impedance of the metal coil is $Z_{\mathrm{m}} = R_{\mathrm{m}} + \mathrm{i}2\pi f L_{\mathrm{m}}$, where R_{m} is the resistance, f is the frequency, L_{m} is the inductance, and $\mathrm{i} = \sqrt{-1}$. When a current, I_{in}, is applied to the metal coil, the power that the metal coil can transduce is $|I_{\mathrm{in}}|^2 2\pi f L_{\mathrm{m}}$. The resistance and the inductance are $R_{\mathrm{m}} = 4\ \Omega$ and $L_{\mathrm{m}} = 0.5$ mH, so that the inductance-to-resistance ratio is $|\mathrm{i}2\pi f L_{\mathrm{m}}/R_{\mathrm{m}}| = 0.39$ at 500 Hz and the energy loss due to Joule heat is $|I_{\mathrm{in}}|^2 R_{\mathrm{m}}$, which is $\frac{R_{\mathrm{m}}}{2\pi f L_{\mathrm{m}} + R_{\mathrm{m}}} = 72\%$ of the input power. By contrast, in a conventional metallic transformer (for example, CKUU16-303-0.4A, Shenzhen Cenker), the resistance and the inductance of the primary metal coil are $2.8\ \Omega$ and 30 mH. Consequently, the inductance-to-resistance ratio is 33.6 at 500 Hz and the energy loss is negligible compared to that of the ionotronic transformer. As the resistance of the hydrogel coil (258 kΩ at 500 Hz) is orders of magnitude higher than that of the metal coil, the energy loss is more significant. As a result, the energy efficiency of the ionotronic transformer is low.

To estimate the energy conversion efficiency of the ionotronic transformer, a resistor, $R_{\mathrm{L}} = 1\ \Omega$, is connected to the hydrogel coil in series. We measure the voltage between the two ends of the metal coil, U_{in}, and the input power is calculated as $U_{\mathrm{in}} I_{\mathrm{in}}$. We also measure the voltage between the two ends of the resistor, U_{out}, and the current through the resistor, I_{out}, so that the output power is calculated as $U_{\mathrm{out}} I_{\mathrm{out}}$. The energy conversion efficiency is defined as $\frac{U_{\mathrm{out}} I_{\mathrm{out}}}{U_{\mathrm{in}} I_{\mathrm{in}}}$. We plot the measured efficiency as a function of I_{out}, which varies with the frequency (Fig. S3). The efficiency reaches 1.8% when $I_{\mathrm{out}} = 0.14$ A.

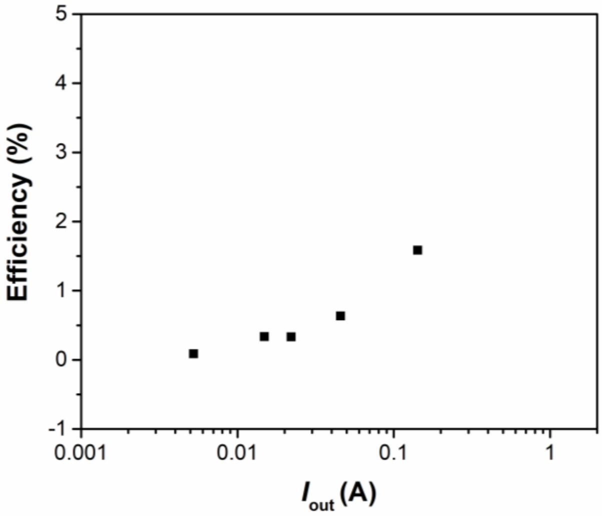

Fig. S3 Energy conversion efficiency of the ionotronic transformer as a function of output current.

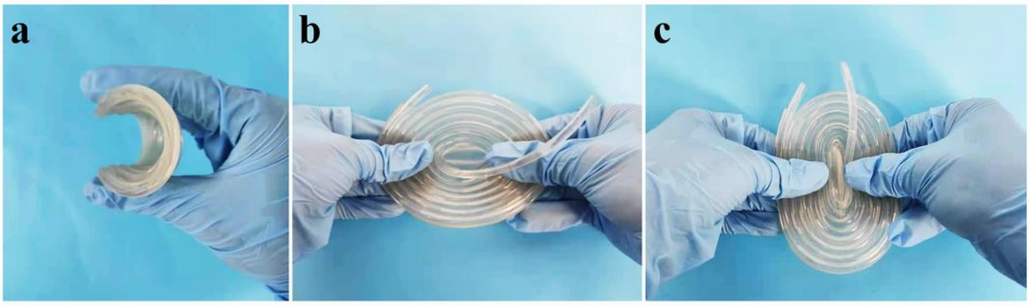

Fig. S4 Photos of soft and flexible hydrogel coil. The hydrogel coil in a bent state (a), stretched state (b), and compressed state (c).